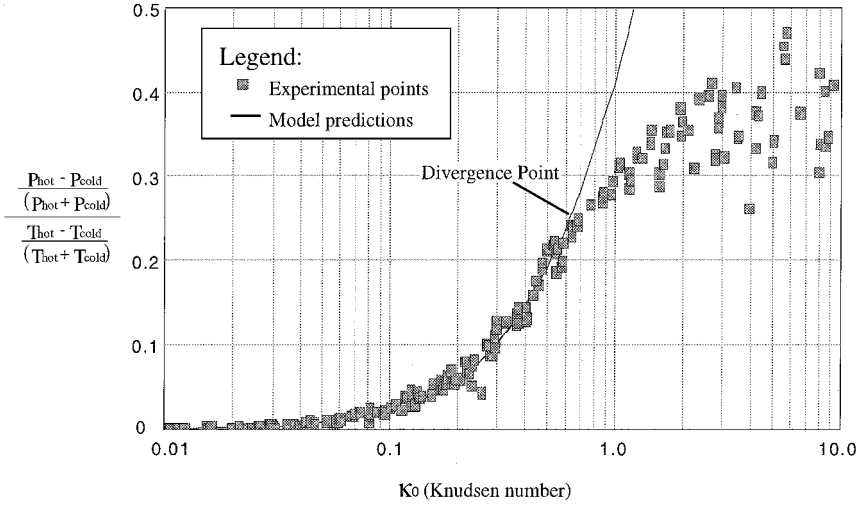

Fig. 3 Comparison of the steady-state model response to experimental results.

Conclusion

This Note reports on the development of a dynamic model for pressure sensing configurations in high Knudsen number flows. The model, applicable to both continuum and rarefied flow conditions, allows for longitudinal temperature gradients in the sensor configuration. The applicable flow regimes for the model were evaluated by a series laboratory tests. Model comparisons are excellent for Knudsen numbers up to 0.65. For values of $\kappa_0 > 0.65$, free molecule effects dominate, and the model is no longer valid. The model represents a fundamental contribution to the understanding of flow behavior at the limits of the continuum flow regime. The model allows instrumentation designers to evaluate the responses of pneumatic systems over a wide range of flow conditions that may vary continuously from continuum to slip-flow. Other potential applications outside of aerospace include predicting the behavior of micromachined fluid systems where the mean free path of the working fluid is on the order of the channel diameter.

References

[1]Lamb, R. C., "The Influence of Geometry Parameters upon Lag Error in Airborne Pressure Measurement Systems," Wright Air Development Center, TR 57-351, Wright–Patterson AFB, OH, July 1957.

[2]Iberall, A. S., "Attenuation of Oscillatory Pressures in Instrument Lines," U.S. National Bureau of Standards, Rept. RP 2115, Vol. 45, Washington, DC, July 1950.

[3]Schuder, C. B., and Binder, R. C., "Response of Pneumatic Transmission Lines to Step Inputs," *Journal of Basic Engineering*, Vol. 81, No. 12, 1959, pp. 578–584.

[4]Hougen, J. O., Martin, O. R., and Walsh, R. A., "Dynamics of Pneumatic Transmission Lines," *Journal of Control Engineering*, Vol. 10, No. 3, 1963, pp. 114–117.

[5]Berg, H., and Tijdeman, H., "Theoretical and Experimental Results for the Dynamic Response of Pressure Measuring Systems," Nat. Luchtavaatlab, NLR-TR F.238, Amsterdam, The Netherlands, Jan. 1965.

[6]Tijdeman, H., "Investigation of the Transonic Flow Around Oscillating Airfoils," Nat. Luchtavaatlab, NLR-TR 77090 U, Amsterdam, The Netherlands, Sept. 1977.

[7]Parrot, T. L., and Zorumski, W., "Sound Transmission Through a High-Temperature Acoustic Probe Tube," *AIAA Journal*, Vol. 30, No. 2, 1992, pp. 318–323.

[8]Maxwell, J. C., "On Stress in Rarefied Gases Arising from Inequalities of Temperature," *Journal of Philosophical Transactions*, Vol. 170, Pt. 1, 1879, pp. 231–235.

[9]von Knudsen, M., "Eine Revision der Gleichgewichtsbedingung der Gase: Thermische Molekularströmung," *Annalen dek Physik*, Vol. 31, Nov. 1910, pp. 205–229.

[10]Tompkins, J., and Wheeler, L., "The Correction for Thermo-Molecular Flow," *Transactions of the Faraday Society*, Vol. 29, Nov. 1933, pp. 1248–1254.

[11]Whitmore, S. A., Petersen, B. J., and Scott, D. D., "A Dynamic Response Model for Pressure Sensors in Continuum and High Knudsen Number Flows with Large Temperature Gradients," NASA TM-4728, Jan. 1996.

[12]Kennard, E. H., *Kinetic Theory of Gases*, McGraw–Hill, New York, 1938, pp. 311–337.

[13]Stephens, R. W. B., and Bate, A. E., *Acoustics and Vibrational Physics*, St. Martin, New York, 1966, pp. 660–682.

[14]Freiberger, W. F. (ed.), *The International Dictionary of Applied Mathematics*, Van Nostrand, Princeton, NJ, 1960, p. 707.

[15]Rade, L., and Westergren, B., *Beta Mathematics Handbook*, CRC Press, Boca Raton, FL, 1994, pp. 287–288.

[16]Doeblin, E. O., *Measurement Systems Application and Design*, McGraw–Hill, New York, 1983, pp. 410–455.

R.P. Lucht
Associate Editor

Postbuckling of Delaminated Composites Under Compressive Loads Using Global–Local Approach

Jun-Sik Kim* and Maenghyo Cho†
Inha University, Inchon 402-751, Republic of Korea

I. Introduction

To describe the damage process of delaminated composites up to final failure, bifurcation buckling analysis might not be enough, and a postbuckling analysis may be required because composite laminates have load-carrying capacity above the buckling loads. Three-dimensional elasticity models[1] or layerwise plate models[2] are adequate to predict postbuckling behaviors of multiple delaminated composite laminates. However, these kinds of analyses require large amounts of computer resources. Thus, for an engineering analysis to save computing time and memory, a global–local analysis is a suitable choice for compromising accuracy and efficiency. However, the postbuckling problems for the laminates with multiple delaminations are not reported in the global–local approaches.

The failure analysis of delaminated plates is quite complicated because it includes postbuckling load increments, iterations of delamination zone propagation, and a contact algorithm between delaminated interfaces. Thus, the numerical analysis of a failure mechanism involves multistep nonlinear iterations. To treat this whole

Received Aug. 10, 1996; presented as Paper 97-1293 at the AIAA/ASME/ASCE/AHS/ASC 38th Structures, Structural Dynamics, and Materials Conference, Kissimmee, FL, April 7–10, 1997; revision received Oct. 20, 1998; accepted for publication Feb. 5, 1999. Copyright © 1999 by the American Institute of Aeronautics and Astronautics, Inc. All rights reserved.

*Graduate Research Assistant, Department of Aerospace Engineering, 253 Yong-Hyun Dong Nam-Ku.

†Assistant Professor, Department of Aerospace Engineering, 253 Yong-Hyun Dong Nam-Ku. Member AIAA.

complexity, efficient modeling for delaminated composites needs to be developed.

Early work for a one-dimensional model was performed by Chai et al.[3] The research of the past 20 years in the delamination buckling/postbuckling field was reviewed extensively by Simitses.[4] Recently, multiple delaminated postbuckling behaviors have been studied based on the finite element method by Lee et al.[5] The objective of the present study is to develop an efficient numerical model that can accurately analyze postbuckling behaviors for laminates with multiple delaminations without a significant increase in the memory size.

A global–local approach for a postbuckling problem with multiple delaminations is presented. A novel transition element between the layerwise element regions and the first-order shear deformation zone is proposed by using a postprocess method. This transition element is easy to implement and performs competently even in thick composites by choosing proper shear correction factors in the first-order model.

II. Formulations

A. Layerwise Model and First-Order Model

An N-layer, fiber-reinforced, composite beam-plate with multiple through-the-width delaminations is considered. To model the multiple delamination, the assumed displacement field is supplemented with unit step functions that allow discontinuities in the displacements, as suggested by Barbero.[6]

The resulting in-plane and out-of-plane displacements U_α and U_3, at a generic point x, y, z in the laminate, are assumed to be in the following form (as in Refs. 7 and 8):

$$U_\alpha(x, y, z) = u_\alpha(x, y) + \sum_{j=1}^{N} \phi^j(z) u_\alpha^j(x, y) + \sum_{i=1}^{D} \delta^i(z) \bar{u}_\alpha^i(x, y)$$

$$U_3(x, y, z) = w(x, y) + \sum_{i=1}^{D} \delta^i(z) \bar{w}^i(x, y)$$

where N is the total number of layers and D is the total number of delaminations. The terms $\bar{u}_\alpha^i$ and $\bar{w}^i$ represent possible jumps in the slipping and opening displacements, respectively, at the $L(i)$th delaminated interface. The $L(i)$ denotes the location of an interface where the ith delamination lies, $\phi^j(z)$ is a linear Lagrangian interpolation function through the thickness of the laminates, and $\delta^i(z)$ is the step function.

Adopting the von Kármán large deflection assumption with initial imperfections, the strain-displacement relations for a one-dimensional beam-plate can then be determined from a layerwise displacement field as

$$\varepsilon_x = \varepsilon_x^o + \sum_{j=1}^{N} \phi^j(z) \varepsilon_x^j + \sum_{i=1}^{D} \delta^i(z) \bar{\varepsilon}_x^i + \sum_{i=1}^{D} \sum_{s=1}^{D} \delta^i(z) \delta^s(z) \bar{\varepsilon}_x^{is}$$

$$\gamma_{xz} = \gamma_{xz}^o + \sum_{j=1}^{N} \phi^j(z) \gamma_{xz}^j + \sum_{i=1}^{D} \delta^i(z) \bar{\gamma}_{xz}^i \tag{1}$$

The constitutive equation and the detailed derivation of the layerwise theory for geometric nonlinearity are given in Ref. 7.

The displacement field of the first-order shear deformation plate theory (FOPT) is given as follows:

$$U_\alpha(x, y, z) = u_\alpha(x, y) + \psi_\alpha(x, y) z, \qquad U_3(x, y, z) = w(x, y) \tag{2}$$

where u_α and w are the midplane stretching and out-of-plane deflection, respectively. The rotational variable ψ_α is the angle of rotation at the midplane.

Considering the von Kármán nonlinearity assumption with initial imperfections, the strain-displacement relations for a one-dimensional beam-plate can then be determined from the FOPT displacement field as

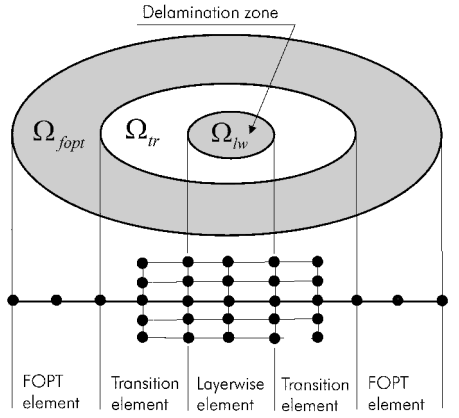

Fig. 1 Definition of the transition domain.

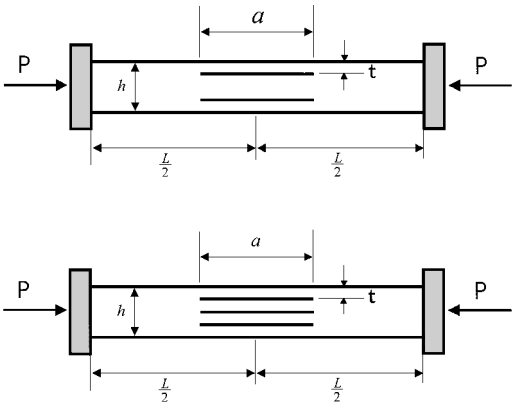

Fig. 2 Geometry of a unidirectional composite with two and three delaminations.

$$\varepsilon_x = u_{,x} + \tfrac{1}{2} w_{,x}^2 + w_{,x} \xi_{,x} + z \psi_{x,x}, \qquad \gamma_{xz} = w_{,x} + \psi_x \tag{3}$$

The constitutive equation and the detailed formulation for geometric nonlinearity are given in Ref. 9

B. Construction of the Relationship Between Layerwise Theory and First-Order Shear Deformation Theory

Consider a domain Ω that is modeled as independently discretized subdomains, $\Omega_{\rm lw}$, $\Omega_{\rm fopt}$, and $\Omega_{\rm tr}$, as shown in Fig. 1. The total potential energy of the system is the sum of the potential energies of subdomains $\Omega_{\rm lw}$, $\Omega_{\rm fopt}$, and $\Omega_{\rm tr}$:

$$\Pi_\Omega = \Pi_{\Omega_{\rm lw}} + \Pi_{\Omega_{\rm fopt}} + \Pi_{\Omega_{\rm tr}}$$

$$\Pi_\Omega = \tfrac{1}{2} \boldsymbol{U}_{\rm lw}^T \boldsymbol{K}_{\rm lw} \boldsymbol{U}_{\rm lw} + \tfrac{1}{2} \boldsymbol{U}_{\rm fopt}^T \boldsymbol{K}_{\rm fopt} \boldsymbol{U}_{\rm fopt} + \tfrac{1}{2} \boldsymbol{U}_{\rm tr}^T \boldsymbol{K}_{\rm tr} \boldsymbol{U}_{\rm tr} \tag{4}$$

$$- \boldsymbol{U}_{\rm lw}^T \boldsymbol{F}_{\rm lw} - \boldsymbol{U}_{\rm fopt}^T \boldsymbol{F}_{\rm fopt} - \boldsymbol{U}_{\rm tr}^T \boldsymbol{F}_{\rm tr}$$

The subscripts lw, tr, and fopt denote layerwise domain, transition domain, and FOPT domain, respectively. The $\boldsymbol{K}$, $\boldsymbol{U}$, and $\boldsymbol{F}$ are the stiffness matrices, the generalized displacement, and the load vector at each domain, respectively; and n is the number of nodes at each domain.

The transition stiffness matrix $\boldsymbol{K}_{\rm tr}^e$ and transition displacement vector $\boldsymbol{U}_{\rm tr}^e$ for each element are calculated from

$$\boldsymbol{K}_{\rm tr}^e = \boldsymbol{T}^{eT} \boldsymbol{K}_{\rm lw}^e \boldsymbol{T}^e, \qquad \boldsymbol{F}_{\rm tr}^e = \boldsymbol{T}^{eT} \boldsymbol{F}_{\rm lw}^e \tag{5}$$

The transformation matrix $\boldsymbol{T}^e$ for each element is calculated from the transverse shear strain relationship between first-order and layerwise theories:

$$w_{,\alpha} + \sum_{j=1}^{N} \phi_{,3}^j u_\alpha^j = c_\alpha^k (w_{,\alpha} + \psi_\alpha)^{\rm fopt} \tag{6}$$

where the matching factor c_α^k is constant at each layer. The determination procedure of the matching factor is omitted here because of limited space; it can be found in Ref. 10.

Using Eq. (6), we obtain the matrix relationship as follows:

$$\begin{bmatrix} c_\alpha^1 N_{1,\alpha}(l) & \cdots & c_\alpha^1 N_{m,\alpha}(l) & c_\alpha^1 \\ c_\alpha^2 N_{1,\alpha}(l) & \cdots & c_\alpha^2 N_{m,\alpha}(l) & c_\alpha^2 \\ \vdots & \ddots & \vdots & \vdots \\ c_\alpha^{N/2} N_{1,\alpha}(l) & \cdots & c_\alpha^{N/2} N_{m,\alpha}(l) & c_\alpha^{N/2} \\ c_\alpha^{N/2+1} N_{1,\alpha}(l) & \cdots & c_\alpha^{N/2+1} N_{m,\alpha}(l) & c_\alpha^{N/2+1} \\ \vdots & \ddots & \vdots & \vdots \\ c_\alpha^{N-1} N_{1,\alpha}(l) & \cdots & c_\alpha^{N-1} N_{m,\alpha}(l) & c_\alpha^{N-1} \\ c_\alpha^{N} N_{1,\alpha}(l) & \cdots & c_\alpha^{N} N_{m,\alpha}(l) & c_\alpha^{N} \end{bmatrix} \begin{Bmatrix} w_1 \\ \vdots \\ w_m \\ \psi_{\alpha l} \end{Bmatrix}$$

$$= \begin{bmatrix} N_{1,\alpha}(l) & \cdots & N_{m,\alpha}(l) & -1/h^1 & 1/h^1 & 0 & \lfloor 0 \rfloor_{N-3} \\ N_{1,\alpha}(l) & \cdots & N_{m,\alpha}(l) & 0 & -1/h^2 & 1/h^2 & \lfloor 0 \rfloor_{N-3} \\ \cdots & & & & & & \\ N_{1,\alpha}(l) & \cdots & N_{m,\alpha}(l) & \lfloor 0 \rfloor_{N/2-1} & -1/h^{N/2} & 0 & \lfloor 0 \rfloor_{N/2-1} \\ N_{1,\alpha}(l) & \cdots & N_{m,\alpha}(l) & \lfloor 0 \rfloor_{N/2-1} & 0 & 1/h^{N/2+1} & \lfloor 0 \rfloor_{N/2-1} \\ \cdots & & & & & & \\ N_{1,\alpha}(l) & \cdots & N_{m,\alpha}(l) & \lfloor 0 \rfloor_{N-3} & -1/h^{N-2} & 1/h^{N-1} & 0 \\ N_{1,\alpha}(l) & \cdots & N_{m,\alpha}(l) & \lfloor 0 \rfloor_{N-3} & 0 & -1/h^{N-1} & 1/h^N \end{bmatrix} \begin{Bmatrix} w_1 \\ \vdots \\ w_m \\ u_{\alpha l}^1 \\ u_{\alpha l}^2 \\ u_{\alpha l}^3 \\ \vdots \\ u_{\alpha l}^{N/2} \\ u_{\alpha l}^{N/2+1} \\ \vdots \\ u_{\alpha l}^{N-2} \\ u_{\alpha l}^{N-1} \\ u_{\alpha l}^{N} \end{Bmatrix} \tag{7}$$

or

$$\boldsymbol{T}_{\text{fopt}}^e \boldsymbol{U}_{\text{tr}}^{*e} = \boldsymbol{T}_{\text{lw}}^e \boldsymbol{U}_{\text{lw}}^{*e} \tag{8}$$

where h^k $(k = 1, \ldots, N)$ is the thickness of each layer, the superscript N is the number of layers, and l is the nodal number.

It is assumed that the out-of-plane deflection w of the layerwise theory is the same as that of FOPT. From Eq. (8), the element transformation matrix $\boldsymbol{T}^e$ is calculated as follows:

$$\begin{bmatrix} \boldsymbol{I} & \{0\} \\ \boldsymbol{T}_{\text{fopt}}^e \end{bmatrix} \boldsymbol{U}_{\text{tr}}^e = \begin{bmatrix} \boldsymbol{I} & [0] \\ \boldsymbol{T}_{\text{lw}}^e \end{bmatrix} \boldsymbol{U}_{\text{lw}}^e \tag{9}$$

$$\boldsymbol{U}_{\text{lw}}^e = \begin{bmatrix} \boldsymbol{I} & [0] \\ \boldsymbol{T}_{\text{lw}}^e \end{bmatrix}^{-1} \begin{bmatrix} \boldsymbol{I} & \{0\} \\ \boldsymbol{T}_{\text{fopt}}^e \end{bmatrix} \boldsymbol{U}_{\text{tr}}^e, \qquad \boldsymbol{U}_{\text{lw}}^e = \boldsymbol{T}^e \boldsymbol{U}_{\text{tr}}^e \tag{10}$$

where $\boldsymbol{T}_{\text{fopt}}^e$ is the $N \times (m + 1)$ matrix, $\boldsymbol{T}_{\text{lw}}^e$ is the $N \times (m + N)$ matrix, and $\boldsymbol{I}$ is the $m \times m$ identity matrix. The $\{0\}$ is the $m \times 1$ vector and $[0]$ is the $m \times N$ zero matrix. The other components of $\boldsymbol{U}_{\text{tr}}^e$ are the same as those of $\boldsymbol{U}_{\text{lw}}^e$.

C. Finite Element Formulation

In the finite element model, the generalized displacements of the layerwise model $(u_\alpha, w, u_\alpha^j, \bar{u}_\alpha^i, \bar{w}_\alpha^i)$ and the first-order shear model $(u_\alpha, w, \psi_\alpha)$ are expressed over each element as a linear combination of the one-dimensional quadratic Lagrangian interpolation functions N_l as follows:

$$\left(u_\alpha, w, u_\alpha^j, \bar{u}_\alpha^i, \bar{w}_\alpha^i\right) = \sum_{l=1}^{m} \left(u_{\alpha l}, w_l, u_{\alpha l}^j, \bar{u}_{\alpha l}^i, \bar{w}_{\alpha l}^i\right) N_l \tag{11}$$

$$(u_\alpha, w, \psi_\alpha) = \sum_{l=1}^{m} (u_{\alpha l}, w_l, \psi_{\alpha l}) N_l \tag{12}$$

where m is the number of nodes per element.

Finite element formulations of nonlinear differential equations yield nonlinear algebraic equations for the finite element mesh:

$$\begin{gathered} [K(a)]\{\boldsymbol{a}\} = \{F\} \\ ([K_L] + [K_{NL}] + [K_I])\{\boldsymbol{a}\} = \lambda \{F\}_{\text{ref}} \end{gathered} \tag{13}$$

where

$$[K(a)] = \sum_e \begin{Bmatrix} \boldsymbol{T}^{eT} [K(a)]_{\text{lw}}^e \boldsymbol{T}^e & \text{for } \Omega_{\text{tr}} \\ [K(a)]_{\text{lw}}^e & \text{for } \Omega_{\text{lw}} \\ [K(a)]_{\text{fopt}}^e & \text{for } \Omega_{\text{fopt}} \end{Bmatrix} \tag{14}$$

$$\{F\} = \sum_e \begin{Bmatrix} \boldsymbol{T}^{eT} \{F\}_{\text{lw}}^e & \text{for } \Omega_{\text{tr}} \\ \{F\}_{\text{lw}}^e & \text{for } \Omega_{\text{lw}} \\ \{F\}_{\text{fopt}}^e & \text{for } \Omega_{\text{fopt}} \end{Bmatrix} \tag{15}$$

The $\{\boldsymbol{a}\}$ is the nodal displacement vector, $[K_L]$ the small displacement stiffness matrix, $[K_{NL}]$ the large displacement matrix that contains terms that are linear or quadratic in $\{\boldsymbol{a}\}$, and $[K_I]$ a stiffness matrix that contains terms related to initial out-of-plane imperfection. The λ is a load factor, and $\{F\}_{\text{ref}}$ is the reference nodal force vector. The $\boldsymbol{T}^e$ is the transformation matrix.

Nonlinear deflections are obtained by solving Eqs. (13) using the Newton–Raphson iteration method. Equation (13) can be replaced with the following two iterative equations:

$$\begin{gathered} [K_T(a)]\{\delta \boldsymbol{a}\} = \lambda \{F\}_{\text{ref}} - [K(a)]\{\boldsymbol{a}\} \\ \{\delta \boldsymbol{a}\}^r = \{\boldsymbol{a}\}^{r+1} - \{\boldsymbol{a}\}^r \end{gathered} \tag{16}$$

where r is the number of iterations. The tangent stiffness matrix $[K_T(a)]$ is

$$[K_T(a)] = \frac{\partial}{\partial \{\boldsymbol{a}\}} ([K(a)]\{\boldsymbol{a}\}) \tag{17}$$

III. Numerical Results and Discussion

To examine the accuracy of the proposed method, a delaminated beam-plate under axial compression is considered. Delamination can be placed in any position along the in-plane direction. The number of delaminations and the size of each delamination are chosen arbitrarily. It is assumed that the lengths of the delaminated zones are not increased when loading is applied. Unilateral contacts between the interface of delaminated zones are considered in the present study to avoid the physically inadmissible buckling mode shape. In the present study, we used the contact algorithm of Ref. 5. Two cases of a composite beam-plate under axial compression were considered: unidirectional and cross-ply composite beam-plate.

A. Unidirectional Composite

An example of a composite with multiple delaminations under axial compression is presented to validate the present method. The material used in this example is a random short-fiber SMC-R50 composite whose properties are as follows:

$$E_{11} = 10.9\,\text{GPa}\ (1.58 \times 10^6\ \text{psi})$$

$$E_{22} = 7.58\,\text{GPa}\ (1.10 \times 10^6\ \text{psi})$$

$$G_{12} = 2.48\,\text{GPa}\ (0.36 \times 10^6\ \text{psi})$$

$$G_{13} = 2.48\,\text{GPa}\ (0.36 \times 10^6\ \text{psi})$$

$$\nu_{12} = 0.31, \qquad \nu_{13} = 0.22$$

The geometric configurations of this example are shown in Fig. 2. Composite laminates containing two delaminations with respect to midplane and three delaminations with an additional one at the midplane are considered. The thickness-to-span ratio h/L is assumed to be $\frac{1}{50}$. Postbuckling analysis is performed for $\bar{a} = 0.3$ and $\bar{t} = 0.125$. The results of a full layerwise model are reproduced here for comparison with the present method.

In this case, initial imperfection shapes are obtained for the lowest bifurcation buckling mode. In Figs. 3 and 4, the results of the present method are compared with those of the full layerwise model. As soon as the laminate is subjected to the applied load, the upper layer tends to deflect upward and opens the upper delamination, and the lower delamination always remains closed. The curves for both the two- and three-delamination composites almost coincide until $P = 0.4$. As the load increases, the laminate deflect downward globally. For the two- and three-delamination composites, the postbuckling mechanism is the same and the global behavior of the composite is similar to that of the one-delamination case.

The total number of degrees of freedom for the layerwise and present models is given in Figs. 3 and 4. In multiple delamination cases, the present method gives reliable results for postbuckling behaviors.

B. Cross-Ply Composite

To investigate the bending–stretching coupling effect and the boundary condition effect, the $[0/90/0/90]_s$ symmetric cross-ply composites containing one delamination at the first layer with clamped–clamped and simply supported ends are considered; each ply has the same thickness. The configuration of a cross-ply composite with a single delamination is given in Fig. 5a.

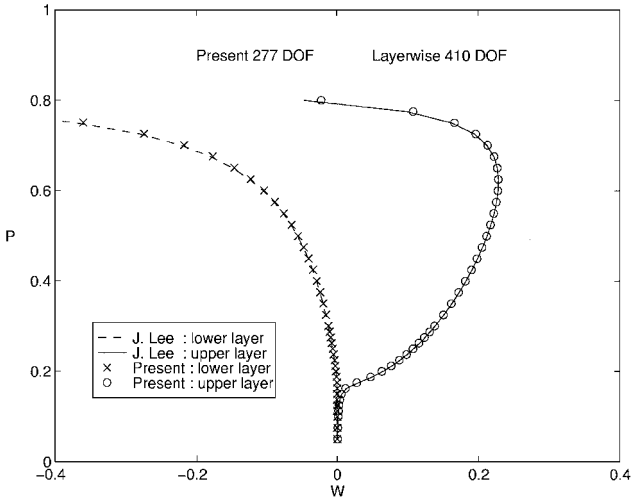

Fig. 3 Load-deflection curve of two-delamination composites.

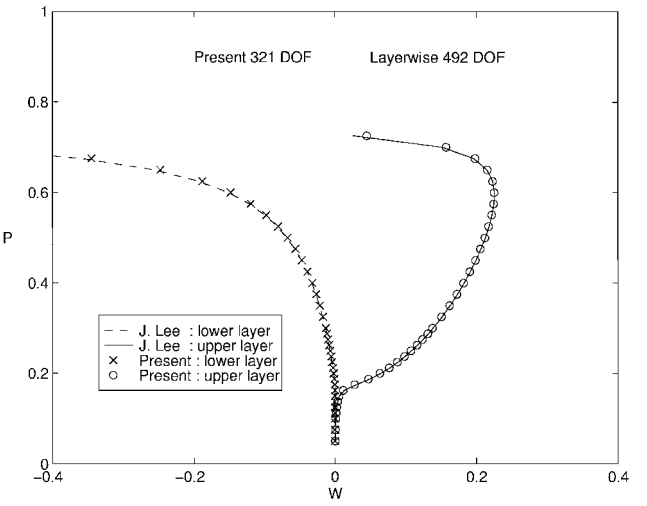

Fig. 4 Load-deflection curve of three-delamination composites.

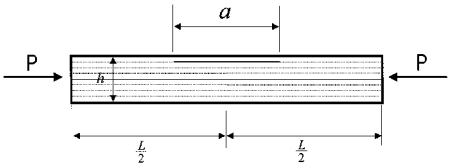

Fig. 5a Geometry of a cross-ply composite with a single delamination.

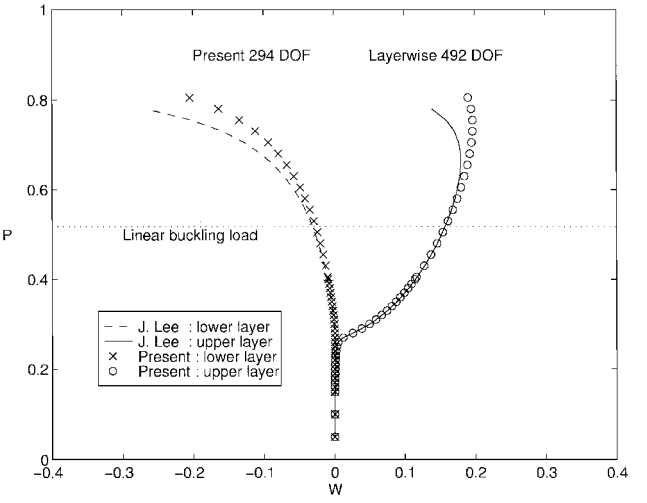

Fig. 5b Load-deflection curve of an $[0/90/90/0]_s$ laminate with clamped ends.

The material used in this example is as follows:

$$E_L = 25 \times 10^6\ \text{psi}, \qquad E_T = 1 \times 10^6\ \text{psi}, \qquad G_{LT} = 0.5 \times 10^6\ \text{psi}$$

$$G_{TT} = 0.2 \times 10^6\ \text{psi}, \qquad \nu_{LT} = \nu_{TT} = 0.25$$

where E, G, and ν represent, respectively, the Young's modulus, the shear modulus, and the Poisson's ratio of the material. The subscripts L and T denote longitudinal and transverse direction, respectively.

The composite laminates are moderately thick ($L/h = 10$), and the delaminated layer is relatively thin ($t/h = 0.125$). For a composite with clamped–clamped ends, the load-deflection curves are shown in Fig. 5b. Because of the delamination, the delaminated region is asymmetric and bending–stretching coupling is present. The initial imperfection is $\xi = \frac{1}{2} w_0 h[1 - \cos(2\pi x/L)]$, $w_0 = 0.001$, and the initial delamination opening is set to zero.

In this case, the postbuckling mechanism is similar to those of the two- and three-delamination cases. However, unlike the

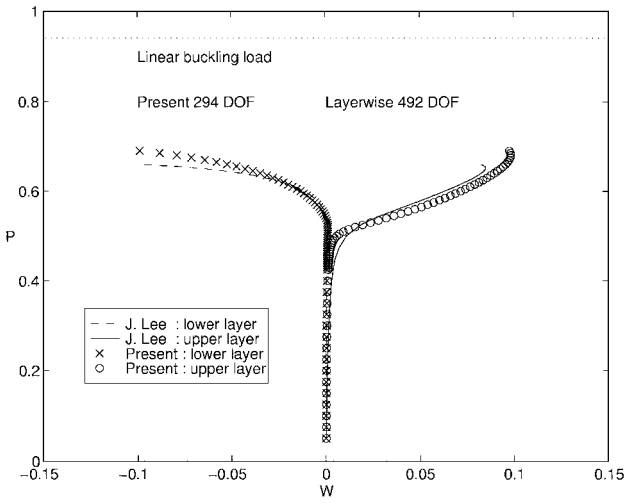

Fig. 5c Load-deflection curve of an $[0/90/90/0]_s$ laminate with simply supported ends.

unidirectional composite, the buckling load calculated from the linear bifurcation analysis is different from that of postbuckling analysis, as shown in Fig. 5b.

For a composite with simply supported ends, the load-deflection curves are shown in Fig. 5c. To satisfy the boundary condition, the initial imperfection is taken as $\xi = w_0 \sin(\pi x/L)$, $w_0 = 0.001$. Once more, the postbuckling response of this case is significantly different from that of the linear bifurcation analysis. In this case, the predicted linear buckling load significantly overestimates the global buckling of the structure.

However, the linear buckling loads may underestimate the global buckling load in the different stacking sequences, as reported in Ref. 5. From this observation, the linear bifurcation buckling loads are quite different from the results of the postbuckling analysis because they depend on the through-the-thickness position of delaminations, the stacking sequence, and the boundary conditions.

For the cross-ply cases, the results of the present global–local method show a slight deviation from those of the full layerwise model as the loads and deflections increase. However, the load-deflection curves of the present method agree reasonably well with those of the layerwise theory and the present model requires a smaller number of degrees of freedom than the layerwise model, as shown in Figs. 5b and 5c.

IV. Conclusions

In the present study, an efficient numerical model was developed to study the postbuckling behaviors of delaminated composites. The analysis was based on the one-dimensional beam-plate model with multiple delaminations.

A global–local approach for postbuckling problems with multiple delaminations was presented. A novel transition element between the layerwise element region and the first-order shear deformation zone was proposed by using a matching technique between first-order and layerwise models. This transition element is easy to implement and performs very well even in thick composites when proper shear correction factors in the first-order model are chosen.

The present numerical model and solution procedure consider the effect of initial imperfections and contact condition between delaminated surfaces. Although accurate postbuckling response can be performed by using layerwise-type theories, they require a great deal of computing time and memory. The proposed global–local method reduces the global degrees of freedom but still accurately models the delaminated zone. Thus it is suitable for the analysis of nonlinear behaviors of multiple delaminated composites.

It is expected that the realistic buckling and postbuckling behaviors of composite laminates with multiple delaminated imbedded cracks can be efficiently analyzed by the present global–local approach. This is now in progress.

Acknowledgment

This research was supported by the 1996 Inha University Research Fund. The authors gratefully acknowledge this support.

References

[1] Whitcomb, J. D., "Finite Element Analysis of Instability Related Delamination Growth," *Journal of Composite Materials*, Vol. 15, Sept. 1981, pp. 403–426.

[2] Reddy, J. N., "A Generalization of Two Dimensional Theories of Laminated Composite Plates," *Communications in Applied Numerical Methods*, Vol. 3, No. 3, 1987, pp. 173–180.

[3] Chai, H., Babcock, C. D., and Knauss, W. B., "One-Dimensional Modeling of Failure in Laminated Plates by Delamination Buckling," *International Journal of Solids and Structures*, Vol. 17, No. 11, 1981, pp. 1069–1083.

[4] Simitses, G. J., "Delamination Buckling of Flat Laminates," *Buckling and Postbuckling of Composite Plates*, edited by G. J. Turvey and I. H. Marshall, Chapman and Hall, London, 1995, pp. 299–328.

[5] Lee, J., Gürdal, Z., and Griffin, O. H., "Postbuckling of Laminated Composites with Delaminations," *AIAA Journal*, Vol. 33, No. 10, 1995, pp. 1963–1970.

[6] Barbero, E. J., "On a Generalized Laminate Plate Theory with Application to Bending, Vibration, and Delamination Buckling in Composite Laminates," Ph.D. Dissertation, Dept. of Engineering Science and Mechanics, Virginia Polytechnic Inst. and State Univ., Blacksburg, VA, Oct. 1989.

[7] Lee, J., "Vibration, Buckling and Postbuckling of Laminated Composites with Delaminations," Ph.D. Dissertation, Dept. of Engineering Science and Mechanics, Virginia Polytechnic Inst. and State Univ., Blacksburg, VA, May 1992.

[8] Cho, M., and Kim, J. S., "Bifurcation Buckling Analysis of Delaminated Composites Using Global-Local Approach," *AIAA Journal*, Vol. 35, No. 10, 1997, pp. 1673–1676.

[9] Chia, C. Y., *Nonlinear Analysis of Plates*, McGraw–Hill, New York, 1980, pp. 96–99.

[10] Kim, J. S., and Cho, M., "Matching Technique of Postprocess Method Using Displacement Fields of Higher Order Plate Theories," *Composite Structures*, Vol. 43, Dec. 1998, pp. 71–78.

G. A. Kardomateas
Associate Editor

Buckling of Filament-Wound Laminated Conical Shells Under Axial Compression

Liyong Tong*
University of Sydney,
Sydney, New South Wales 2006, Australia

Nomenclature

D_{ij} = terms in bending stiffness matrix
M_x = longitudinal bending moment
N_x = longitudinal membrane stress resultant
U = longitudinal displacement
V = circumferential displacement
W = transverse displacement
α = semivertex angle of the conical shell
θ = angle of fiber tow to the slant longitudinal direction in filament winding

I. Introduction

THE buckling behavior of isotropic and orthotropic conical shells under axially compressive loads and/or combined loads has been studied experimentally and analytically by many researchers.[1–7] However, for laminated composite conical shells there has been very limited literature available on experimental and analytical investigation of buckling behavior of composite laminated shells.[8–10] In this study, an experimental investigation is presented to discuss the buckling behavior of nine carbon-fiber-reinforced

Received Feb. 20, 1998; presented as Paper 98-1769 at the AIAA/ASME/ASCE/AHS/ASC 39th Structures, Structural Dynamics, and Materials Conference, Long Beach, CA, April 20–23, 1998; revision received Jan. 8, 1999; accepted for publication Feb. 5, 1999. Copyright © 1999 by the American Institute of Aeronautics and Astronautics, Inc. All rights reserved.

*Senior Lecturer, Department of Aeronautical Engineering. Member AIAA.